

Refractive distortions of partially coherent beams in inhomogeneously absorbing (amplifying) media

V V Dudorov, V V Kolosov, O A Kolosova

Abstract. Based on the equation for the second-order coherence function, the propagation of partially coherent radiation is studied under the combined action of diffraction and refraction caused by the inhomogeneous distribution of the real and imaginary parts of the perturbation of the permittivity of a medium in the case of inhomogeneous absorption (amplification). The limits of application of the method of geometrical optics for inhomogeneously absorbing (amplifying) media are studied, as well as of the methods that neglect refraction caused by the inhomogeneous distribution of the imaginary part of the permittivity of the medium.

Keywords: partially coherent radiation, refraction, diffraction, inhomogeneous absorption, ray methods, geometrical optics.

1. Introduction

The problem of studying the propagation of partially coherent radiation in inhomogeneously absorbing (amplifying) media arises in investigations of the propagation of optical radiation in an absorbing plasma, in studies of the formation of the output radiation of X-ray and other superradiance lasers, in the propagation of laser radiation in bleaching channels, etc. Analytic approaches to this problem are based on the determination of the response function of the medium [1–6] or on the expansion of the solution in eigenmodes [7, 8]. Numerical methods were also widely applied for solving this problem. One of the approaches is based on the Monte Carlo method [9]. This approach is rather universal and does not require any physical limitations or approximations. Its drawback is cumbersome calculations.

Another numerical method based on the numerical solution of the equation for the coherence function gave both analytic and numerical solutions [10, 11]. However, the numerical algorithm in Refs [10, 11] was used for the solution of not an exact but approximate equation for the second-order coherence function, this equation being

Fourier-conjugate to the equation of radiation transfer. It was shown in Ref. [12] that the approximate equation neglects the bending of ray trajectories caused by the inhomogeneity of the imaginary part of the permittivity and, hence, this approach cannot be generalised to strongly absorbing media.

The use of conventional methods of geometrical optics for strongly absorbing media [13] is limited by the region of its applicability. Analytic solutions can be obtained by these methods only for a limited number of distributions of the complex permittivity.

To study the propagation of partially coherent radiation in inhomogeneously absorbing (amplifying) media, we proposed [14] the ray method for solving the equation for the second-order coherence function (method of diffraction rays). Diffraction rays represent trajectories in space, tangents to them at each point being coincident with the direction of the energy flux (the Umov–Poynting vector). This method has two substantial features compared to other ray methods.

First, the solution is based on the use of not geometro-optical rays but of ray trajectories, which are determined taking into account diffraction effects. Second, by applying this method to strongly absorbing media, it is possible to avoid the introduction of complex ray trajectories (unlike other ray methods [13]). The complex trajectories are mathematical abstractions and have no physical meaning. Moreover, they do not contain a complete information, which is required for the construction of real ray trajectories, and do not yield the shape of the radiation intensity distribution.

The advantage of our method is that the numerical algorithms developed on its basis are highly efficient and allow one to study within a single approach the dependence of the energy and coherent characteristics of radiation on all physical phenomena accompanying the propagation of random waves in random linear and nonlinear media [diffraction, refraction, inhomogeneous absorption (amplification), and turbulent broadening of a beam].

2. Ray method for equation solving

The equation for the second-order coherence function $\Gamma_2(z, \mathbf{r}_1, \mathbf{r}_2) = \langle E(z, \mathbf{r}_1)E^*(z, \mathbf{r}_2) \rangle$ can be written in the form [8]

$$2ik \frac{\partial \Gamma_2}{\partial z} + (\Delta_{\perp 1} - \Delta_{\perp 2})\Gamma_2 + k^2 [\Delta \varepsilon(z, \mathbf{r}_1) - \Delta \varepsilon^*(z, \mathbf{r}_2)]\Gamma_2(z, \mathbf{r}_1, \mathbf{r}_2) = 0,$$

V V Dudorov, V V Kolosov Institute of Atmospheric Optics, Siberian Division, Russian Academy of Sciences, Akademicheskii prosp. 1, 634055 Tomsk, Russia; e-mail: kvv@iao.ru; dvv@iao.ru

O A Kolosova Tomsk State University, prosp. Lenina 36, 634050 Tomsk, Russia

Received 7 February 2001

Kvantovaya Elektronika 31 (9) 787–793 (2001)

Translated by M N Sapozhnikov

where $\Delta_{\perp i}$ is the transverse Laplacian; k is the wave number; z is the coordinate along the propagation direction of radiation; \mathbf{r}_1 and \mathbf{r}_2 are the radius vectors in the plane perpendicular to the propagation direction of radiation; $\Delta\varepsilon(z, \mathbf{r}) = \varepsilon(z, \mathbf{r}) + i\sigma(z, \mathbf{r})$ is the perturbation of the complex permittivity of a medium; and $E(z, \mathbf{r})$ is the electromagnetic field.

After the passage to sum and difference coordinates $\mathbf{R} = (\mathbf{r}_1 + \mathbf{r}_2)/2$ and $\boldsymbol{\rho} = \mathbf{r}_1 - \mathbf{r}_2$, the equation for the coherence function takes the form

$$\frac{\partial \Gamma_2}{\partial z} + \frac{1}{ki} \nabla_{\mathbf{R}} \nabla_{\boldsymbol{\rho}} \Gamma_2 + \frac{k}{2i} \left[\Delta\varepsilon \left(z, \mathbf{R} + \frac{\boldsymbol{\rho}}{2} \right) - \Delta\varepsilon^* \left(z, \mathbf{R} - \frac{\boldsymbol{\rho}}{2} \right) \right] \times \Gamma_2(z, \mathbf{R}, \boldsymbol{\rho}) = 0, \tag{1}$$

where $\nabla_{\mathbf{R}}$ and $\nabla_{\boldsymbol{\rho}}$ are transverse gradients over sum and difference coordinates, respectively.

We will use the only assumption that the Gaussian shape of the coherence function over the difference coordinate is preserved, which corresponds to the parabolic surface of the mean phase front over the length equal to the coherence radius, and represent the coherence function in the form

$$\Gamma_2(z, \mathbf{R}, \boldsymbol{\rho}) = \gamma(z, \mathbf{R}, \boldsymbol{\rho}) e^{i\Phi(z, \mathbf{R}, \boldsymbol{\rho})}.$$

From equation (1), we obtain the system of ray equations

$$\frac{d^2 \mathbf{R}}{dz^2} = \frac{1}{2} \nabla_{\mathbf{R}} \varepsilon + \frac{1}{k^2 W} (\nabla_{\boldsymbol{\rho}} \nabla_{\mathbf{R}} \nabla_{\boldsymbol{\rho}} \gamma) \Big|_{\boldsymbol{\rho}=0}, \tag{2}$$

$$\frac{d^2 \boldsymbol{\rho}}{dz^2} = \boldsymbol{\rho} \nabla_{\mathbf{R}} \left[\frac{1}{2} \nabla_{\mathbf{R}} \varepsilon + \frac{1}{k^2 W} (\nabla_{\boldsymbol{\rho}} \nabla_{\mathbf{R}} \nabla_{\boldsymbol{\rho}} \gamma) \Big|_{\boldsymbol{\rho}=0} \right], \tag{3}$$

$$\tau(z, \mathbf{R}(z)) = k \int_0^z dz' \sigma(z', \mathbf{R}(z')), \tag{4}$$

$$\gamma(z, \mathbf{R}, \boldsymbol{\rho}) = \frac{\gamma_0(\mathbf{R}_0, \boldsymbol{\rho}_0)}{|\mathbf{d}\mathbf{R}/\mathbf{d}\mathbf{R}_0|} \times \exp \left[-\tau(z, \mathbf{R}(z)) - \frac{1}{2} \left(\frac{\boldsymbol{\rho}}{2} \nabla_{\mathbf{R}} \right)^2 \tau(z, \mathbf{R}(z)) \right], \tag{5}$$

where γ is the modulus of the coherence function; $W = \gamma(z, \mathbf{R}, \boldsymbol{\rho} = 0)$ is the average radiation intensity; $\gamma_0 = \gamma(z = 0)$; $\mathbf{R}_0 = \mathbf{R}(z = 0)$; and $\boldsymbol{\rho}_0 = \boldsymbol{\rho}(z = 0)$. Equation (2) is the equation for a diffraction ray whose direction at each point coincides with the direction of the average Umov–Poynting vector $\mathbf{d}\mathbf{R}/dz = k^{-1} \nabla_{\boldsymbol{\rho}} \Phi \Big|_{\boldsymbol{\rho}=0}$.

The method of diffraction rays and the analytic solutions for the parabolic distribution of the complex permittivity of the medium obtained by this method are described in more detail in Ref. [14]. The range of applicability of this method was studied in Ref. [15] by comparing its results with exact solutions of the equation for the coherence function. Here, we study numerically the propagation of partially coherent radiation in inhomogeneous media.

3. Refraction in inhomogeneously absorbing media

To use the methods based on the determination of the response function of the medium, it is necessary to know the analytic form of this function. In the problems of

propagation of partially coherent radiation in inhomogeneous media, the response function can be written only in the case of the parabolic distribution of the permittivity. The set of ray equations (2)–(5) can be numerically solved for an arbitrary distribution of the complex permittivity. We used the method having the second-order convergence in the evolution variable, in which the derivatives with respect to the transverse coordinate are calculated using finite differences. The PC-486DX computer time for the calculation of one variant of the problem was from 5 to 30 s for axially symmetric problems and from 1 to 20 min for problems with an arbitrary geometry. These results allow us to compare the solution of the problem of propagation of partially coherent radiation in inhomogeneous media obtained by the method of diffraction rays with the solution obtained in the aberration-free (near-axial) approximation based on the replacement of the distribution of the permittivity of the medium by a parabola coinciding with the distribution $\Delta\varepsilon(z, \mathbf{R}) = (\varepsilon_2 + i\sigma_2) \mathbf{R}^2$ of the permittivity on the ray axis.

Fig. 1a shows the distribution of the average intensity of a partially coherent Gaussian beam propagated through an inhomogeneous medium with a Gaussian transverse distribution of the complex permittivity. One can see that the difference between the solution of the problem obtained by the method of diffraction rays and the solution obtained in the aberration-free approximation increases with increasing the diffraction parameter, which is equal to the ratio of the refraction length $L_r = (\varepsilon_2^2 + \sigma_2^2)^{-1/4}$ to the diffraction length $L_d = ka_0/(a_0^{-2} + a_c^{-2})^{1/2}$ (where a_0 and a_c are the initial radii of the beam and coherence). Fig. 1b shows the relative error of calculation of the intensity on the beam axis in the aberration-free approximation as a function of the evolution variable z/L_r . Note that the intensities differ not only on the axis but also over the entire cross section, resulting in a

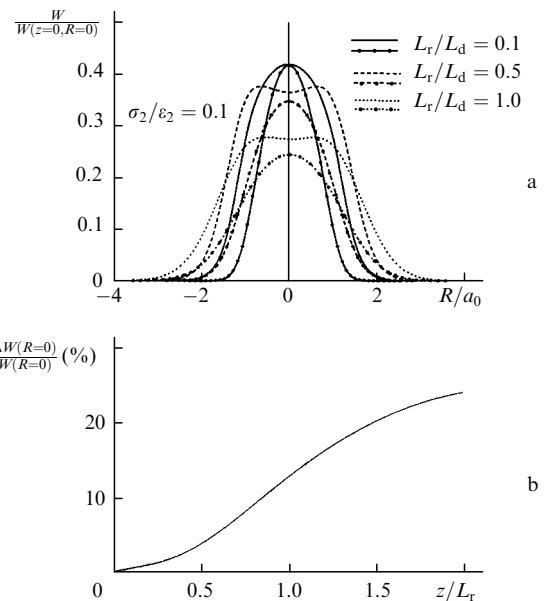


Figure 1. Distributions of the average intensity of a partially coherent Gaussian beam in a medium with $\Delta\varepsilon(z, \mathbf{R}) = (\varepsilon_2 + i\sigma_2)[1 - \exp(-\mathbf{R}^2)]$ calculated in the aberration-free approximation (curves with dots) and by the method of diffraction beams (curves without dots) (a) and the dependence of the relative error of calculation of the average intensity in the aberration-free approximation on the evolution variable z/L_r (b).

substantial increase in the difference between the transmitted and absorbed powers of the beam with increasing z/L_r .

This study showed that in some problems, where the perturbation of the complex permittivity of the medium has a complex non-parabolic form, the aberration-free approximation introduces a significant error to the exact solution.

Another, less stringent approximation, which is used in these problems, involves the solution of the equation for the coherence function, when the bending of the rays caused by the inhomogeneity of the absorption coefficient is neglected assuming that the ratio of the real part of the perturbation to the imaginary one is $\eta = \varepsilon_2/\sigma_2 \gg 1$ [10, 11]. The same refraction is neglected within the framework of the Wentzel–Kramers–Brillouin method used for the determination of the response function of a medium [16]. However, when the condition $\eta \gg 1$ is not valid, the solutions obtained in this approximation differ from exact solutions even for the parabolic distribution of the permittivity. This raises the question of finding the region where the neglect of refraction in the inhomogeneous absorbing medium introduces only an insignificant error to the solution of the problem.

For this purpose, we compared the exact analytic solution of the problem of propagation of partially coherent radiation having the parabolic distribution of the complex permittivity over the beam cross section with an approximate solution in which the refraction caused by inhomogeneous absorption is neglected. The solid curves in Fig. 2 show the ray trajectories for a Gaussian beam propagating in the medium with the parabolic distribution of the permittivity calculated by neglecting the ray-trajectory bending caused by the inhomogeneous distribution of the imaginary part of the permittivity. The dashed curves

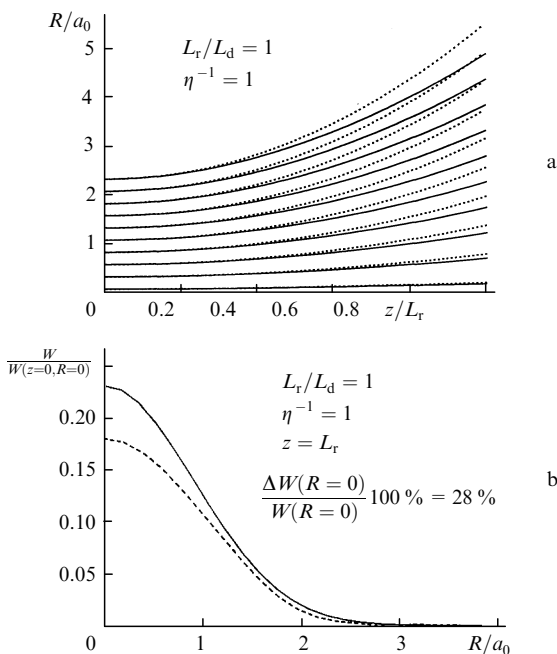


Figure 2. Comparison of ray trajectories calculated by neglecting the ray-trajectory bending caused by inhomogeneous absorption (solid curves) with exact solutions (dashed curves) for $\eta^{-1} = L_r/L_d = 1$ (a); distribution of the radiation intensity calculated by neglecting the ray-trajectory bending caused by inhomogeneous absorption (solid curve) and the exact solution (dashed curve) (b).

show the exact solution. It is obvious that inhomogeneous absorption strongly affects the ray trajectories, resulting in the additional refraction of radiation.

Fig. 2b shows the radiation intensity distribution calculated by neglecting the additional refraction caused by inhomogeneous absorption (the solid curve) and the exact solution of the propagation problem (the dashed curve). One can see that even for the axial beam, where absorption is absent, the intensity calculated by neglecting refraction caused by inhomogeneous absorption noticeably differs from the exact intensity. This is explained by a stronger broadening of the beam, in particular, in the near-axial region, which is caused by the additional bending of the ray trajectories.

Fig. 3 shows the relative error of calculation of the radiation intensity by neglecting the refraction caused by the inhomogeneous distribution of the imaginary part of the perturbation of the permittivity of the medium as a function of the parameter $\eta^{-1} = \sigma_2/\varepsilon_2$. This dependence was calculated for the axial beam with the ratio $L_r/L_d = 0.01, 0.1$, and 1 and the propagation distance $z = L_r$ and $1.5L_r$. One can see that the effect of refraction on the radiation intensity distribution decreases with decreasing the diffraction parameter L_r/L_d . Fig. 4 shows the radiation intensity of the axial ray and the relative error of its calculation by neglecting the bending of ray trajectories caused by inhomogeneous absorption as functions of the evolution variable z/L_r for the parameter $\eta^{-1} = 0.1$ and 0.2. One can see that the relative error of the intensity calculation is rather high even for quite small parameters η^{-1} .

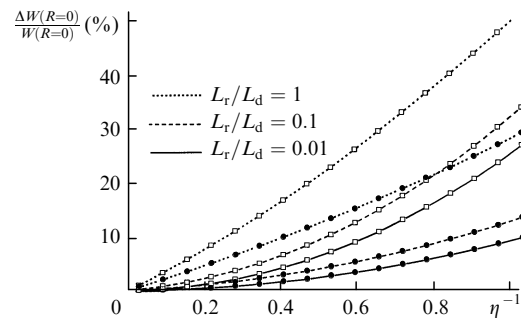


Figure 3. Relative errors of the average radiation intensity of the axial beam calculated by neglecting refraction caused by inhomogeneous absorption as functions of the parameter $\eta^{-1} = \sigma_2/\varepsilon_2$ for the distance $z = L_r$ (●) and $1.5L_r$ (□) and different diffraction parameters L_r/L_d .

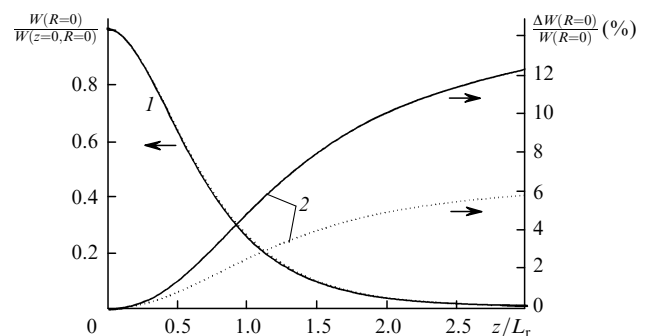


Figure 4. Dependences of the average radiation intensity on the axis (1) and of the relative error of its calculation (2) on the evolution variable z/L_r for $\eta^{-1} = 0.1$ (solid curves) and 0.2 (dashed curves) for $L_r/L_d = 1$.

A similar difference between the solutions obtained by neglecting the refraction caused by inhomogeneous absorption and taking it into account was also observed for other distributions of the permittivity over the beam cross section. Fig. 5a shows the ray trajectories for a Gaussian beam propagating in a medium with a Gaussian distribution of the permittivity. One can see that the rays gradually approach each other with increasing distance, resulting in the peaks in the radiation intensity distribution (Fig. 5b). The dashed curve in Fig. 5b shows the radiation intensity distribution calculated by neglecting the bending of ray trajectories caused by inhomogeneous absorption.

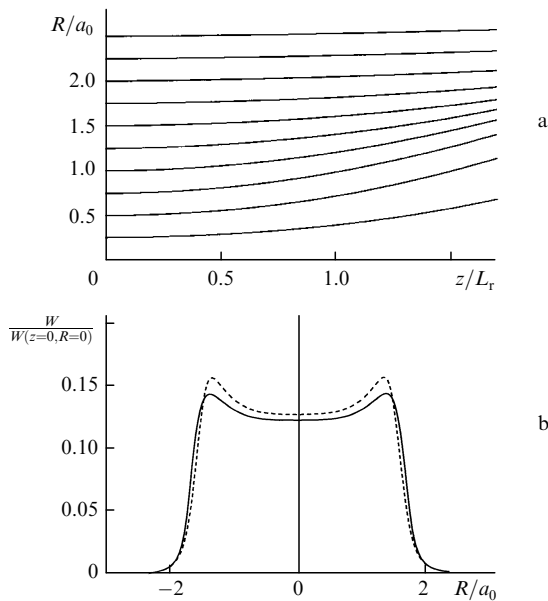


Figure 5. Ray trajectories (a) and distributions of the average radiation intensity calculated, taking into account (solid curve) and neglecting (dashed curve) the ray-trajectory bending caused by inhomogeneous absorption (b), for a Gaussian beam propagating in a medium with a Gaussian distribution of the permittivity $\Delta\varepsilon(z, \mathbf{R}) = (\varepsilon_2 + i\sigma_2)[1 - \exp(-R^2)]$ for $\eta^{-1} = 0.1$ and $L_r/L_d = 0.1$.

Fig. 6 shows the corresponding solutions for a Gaussian beam propagating in a medium with a power distribution of the permittivity. In the absence of refraction caused by inhomogeneous absorption, the rays gradually bend and enter a strongly absorbing region. This is accompanied by a drastic decrease in the intensity distribution in the region of strong absorption (the dashed curve in Fig. 6b). However, when the bending of the ray trajectories caused by inhomogeneous absorption is taken into account, the focusing of the rays is observed (Fig. 6a), which gives rise to the intensity peaks (the solid curve in Fig. 6b) [17]. This can be explained by a combined action of diffraction and refraction on the ray trajectories. Refraction causes the deviation of the rays from the axis to the region of strong absorption. Absorption produces strong gradients in the intensity distribution, which in turn enhance diffraction bending of the rays. The bent rays enter the region of strong refraction, and the process becomes self-consistent. We emphasise that the refraction caused by the inhomogeneity of the imaginary part of the permittivity of the medium noticeable affects the intensity distribution already for $\eta^{-1} = 0.1$.

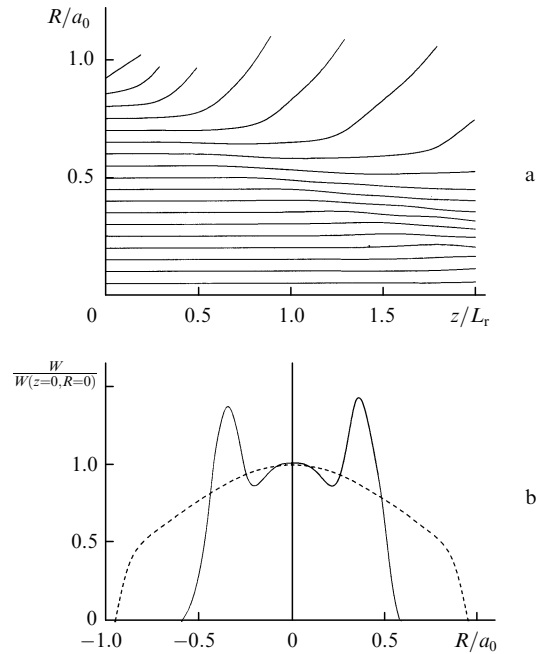


Figure 6. Ray trajectories (a) and distributions of the average radiation intensity calculated, taking into account (solid curve) and neglecting (dashed curve) the ray-trajectory bending caused by inhomogeneous absorption (b), for a Gaussian beam propagating in a medium with a power distribution of the permittivity $\Delta\varepsilon(z, \mathbf{R}) = (\varepsilon_2 + i\sigma_2)\mathbf{R}^{20}$ for $\eta = 0$.

The results obtained above show that in calculations of the propagation of radiation in inhomogeneous media where the perturbation of the imaginary part of the permittivity is comparable with the real part, one should take into account the refraction caused by the inhomogeneity of the imaginary part.

4. Limits of applicability of the geometrical optics approximation for inhomogeneously absorbing media

Another approximate approach to the solution of the problems under study is geometrical optics. Traditionally, it is based on complex ray trajectories, amplitudes, and caustics [13]. The system of ray equations (2)–(5) yields, upon the passage to the limit $k \rightarrow \infty$ (in the geometrical optics approximation), the equation

$$\frac{d^2 \mathbf{R}}{dz^2} = \frac{1}{2} \nabla_{\mathbf{R}} \left\{ \varepsilon(z, \mathbf{R}(z)) + \frac{1}{4} \left[\int_0^z dz' \nabla_{\mathbf{R}} \sigma(z', \mathbf{R}(z')) \right]^2 \right\}, \quad (6)$$

for a trajectory of a real ray, where $\Delta\varepsilon(z, \mathbf{R}) = \varepsilon(z, \mathbf{R}) + i\sigma(z, \mathbf{R})$ is the perturbation of the complex permittivity of the medium.

Equation (6) differs from the geometrical-optics equation for homogeneously absorbing media by the presence of the second term in its right-hand side. This term depends on the spatial distribution of the imaginary part of the permittivity. This distribution considerably differs from the dependence of the first term on the real part of the permittivity.

The first difference is related to the quadratic dependence of the second term on the imaginary part of the permittivity. This means that the behaviour of the ray

trajectory in the geometrical-optics limit is independent of the sign of σ , i.e., for the same dependence of σ on spatial coordinates, the ray trajectories behave in the same way, both in amplifying and absorbing media. Note, however, that this does not mean that radiation propagates identically in these media, because in the first case the radiation is amplified along the chosen ray trajectories, whereas in the second case, it decays.

Another difference is related to the fact that the second term in (6) vanishes not only in media with the homogeneous distribution of σ over the cross section but also in media where the transverse gradient of the imaginary part of the permittivity is constant ($\nabla_{\mathbf{R}}\sigma = \text{const}$), i.e., this term plays a role only in the media where the distribution of the imaginary part of the permittivity has nonzero second derivatives with respect to transverse coordinates.

The presence of the integral term in the right-hand side of equation (6) means that this equation is not a second-order differential equation. Therefore, the two initial conditions, namely, the position of the initial point and the value of the slope are insufficient for determining a trajectory of a real ray. Therefore, we can conclude that the trajectory of a ray in the medium with the inhomogeneous absorption coefficient depends not only on the distribution of the complex permittivity but also on the wave-front curvature. In this case, the rays emerging from a point in space at the same direction, but belonging to the wave fronts with different curvatures in the vicinity of this point will propagate along different trajectories because the behaviour of the rays surrounding the given ray changes. This is a fundamental difference between the geometrical optics of inhomogeneously absorbing media and the geometrical optics of homogeneously absorbing media.

This can be illustrated by the example of the exact analytic solution of the problem of propagation of coherent radiation in a medium with the parabolic perturbation profile of the complex permittivity [14]. Fig. 7 shows the ray trajectories for the rays belonging to the beams with different wave fronts, spherical and plane. We should take into account that for the beams from an infinite set of pairs of rays emerging from one point, the coincidence of the initial slopes is possible only for one pair. The ray trajectories for this pair are shown in Fig. 7 by solid curves. While the rays emerged from one point in the direction shown by the arrow first propagate along close trajectories, the trajectories of these rays gradually become substantially

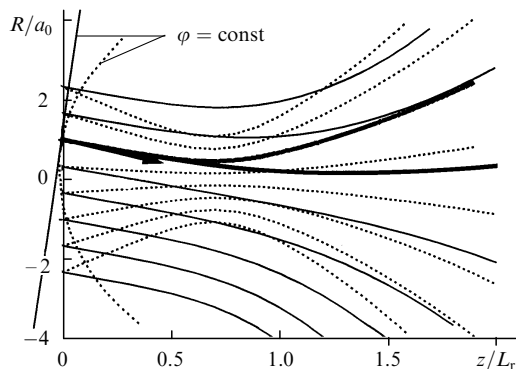


Figure 7. Ray trajectories for sets of rays belonging to the beams with spherical (dashed curves) and plane (solid curves) wave fronts (φ is the wave phase).

different with increasing distance and, hence, with the enhancement of the effect of refraction caused by inhomogeneous absorption.

Let us find now the region of applicability of simple methods of geometrical optics.

Based on the analytic solutions for the parabolic distribution of the complex permittivity of the medium and the numerical simulation of the medium with an arbitrary distribution of the permittivity, we compared the solutions obtained in the geometrical optics approximation with exact solutions. We analysed the propagation of optical radiation for three different axially symmetric distributions of the complex permittivity of the medium: parabolic $\Delta\varepsilon(z, \mathbf{R}) = (\varepsilon_2 + i\sigma_2)\mathbf{R}^2$, Gaussian $\Delta\varepsilon(z, \mathbf{R}) = (\varepsilon_2 + i\sigma_2)[1 - \exp(-\mathbf{R}^2)]$, and power $\Delta\varepsilon(z, \mathbf{R}) = (\varepsilon_2 + i\sigma_2)\mathbf{R}^{20}$. Upon propagation of a Gaussian beam through a medium with the parabolic distribution of the permittivity, the exact solution converges to the solution constructed for rays for the distance of the order of $z = 2L_r$ already at $L_r/L_d = 0.1$. This convergence of the solutions takes place both for coherent and partially coherent radiation. Fig. 8a presents the solutions of the problem of propagation of partially coherent radiation for $\eta^{-1} = 1$, $z = 2L_r$ and the diffraction parameter $L_r/L_d = 0.1, 0.3$, and 0.5 . Fig. 8b shows the relative error of calculation of the radiation intensity for the axial ray in the geometrical optics approximation as a function of the parameter L_r/L_d for distances $z = 1.5L_r$ and $2L_r$. These dependences were obtained for coherent and partially coherent radiation for the ratios of the initial coherence radius to the initial beam radius $a_c/a_0 = 1$ and lower than 0.2 . Similar results were obtained for the Gaussian (Fig. 9) and power (Fig. 10) distributions of the permittivity of the medium.

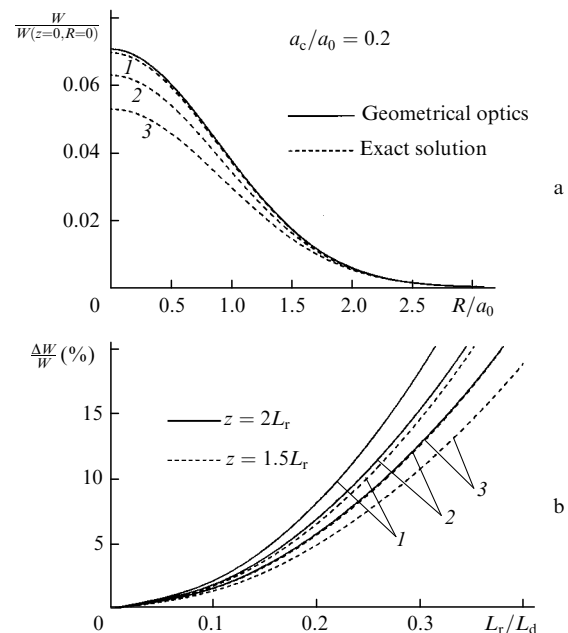


Figure 8. Distributions of the average intensity of a partially coherent Gaussian beam in a medium with $\Delta\varepsilon(z, \mathbf{R}) = (\varepsilon_2 + i\sigma_2)\mathbf{R}^2$ for $L_r/L_d = 0.1$ (1), 0.3 (2), and 0.5 (3) (a) and dependences of the relative error of calculation of the average radiation intensity of the axial ray in the geometrical optics approximation on the diffraction parameter for coherent (1) and partially coherent radiation for $a_c/a_0 = 1$ (2) and $a_c/a_0 \leq 0.2$ (3) (b).

Fig. 9a shows the distributions of the radiation intensity for a Gaussian beam propagating through a medium with a Gaussian distribution of the permittivity at the distance $z = 2L_r$ for $\eta^{-1} = 1$ and three diffraction parameters $L_r/L_d = 0.01, 0.05,$ and 0.1 . For $L_r/L_d = 0.01$, the intensity distributions for coherent and partially coherent beams coincided with the distribution obtained in the geometrical optics approximation. The difference between the intensity distributions increased with increasing diffraction parameter. Note that the difference of the intensity distribution for partially coherent radiation from the geometrical optics distribution is smaller than that for coherent radiation. Fig. 9b shows the dependence of the relative error of calculation of the intensity radiation in the aberration maximum on the diffraction parameter L_r/L_d for the distance $z = 2L_r$. Note that for the same range of variation of the diffraction parameter at the distance $z = 1.5L_r$, the error of calculation of the radiation intensity in the geometrical optics approximation is less than one per cent. Fig. 10a shows the distribution of the radiation intensity for a Gaussian beam propagating through a medium with a power distribution of the permittivity at the distance $z = 2L_r$ for $\eta^{-1} = 1$. Fig. 10b presents the relative error of calculation of the intensity of coherent radiation in the first aberration maximum in the geometrical optics approximation as a function of the diffraction parameter. Note that the relative error of calculation of the intensity of partially coherent radiation for the ratio $a_c/a_0 < 0.2$ (Fig. 10c) is an order of magnitude lower than the relative error for coherent radiation for the same diffraction parameter.

Therefore, the ray solution converges to the exact solution for partially coherent radiation faster than for

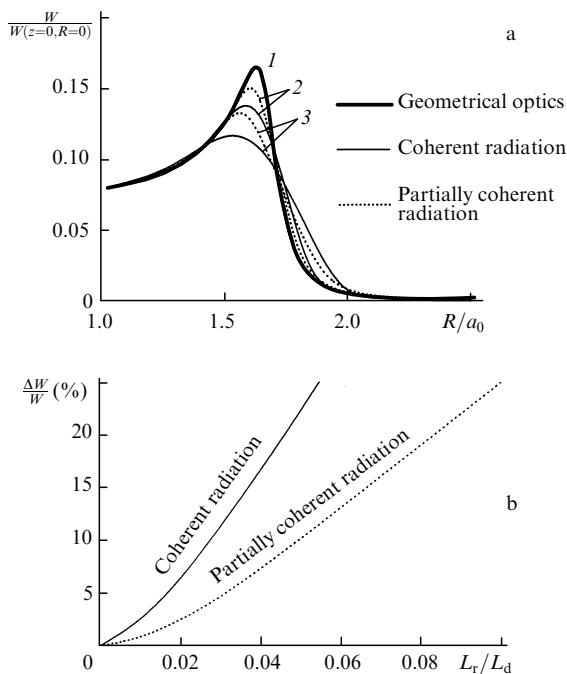


Figure 9. Distributions of the average intensity of coherent and partially coherent Gaussian beams in a medium with $\Delta\epsilon(z, \mathbf{R}) = (\epsilon_2 + i\sigma_2)[1 - \exp(-R^2)]$ for $L_r/L_d = 0.01$ (1), 0.05 (2), and 0.1 (3) (a) and dependences of the relative error of calculation of the average radiation intensity at the aberration maximum in the geometrical optics approximation on the diffraction parameter (b).

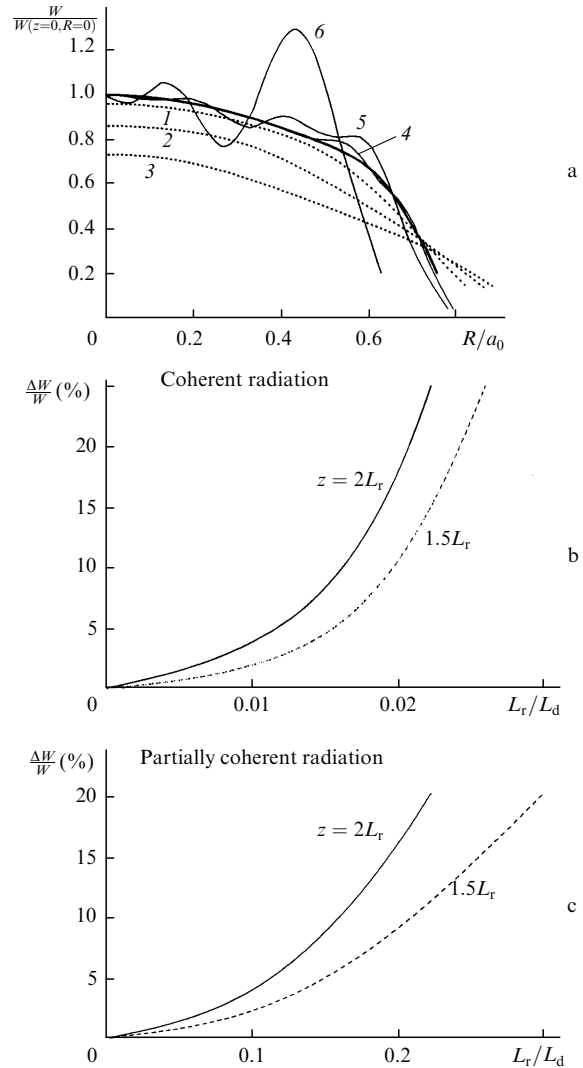


Figure 10. Distributions of the average intensity of partially coherent (1–3) and coherent (4–6) Gaussian beams in a medium with $\Delta\epsilon(z, \mathbf{R}) = (\epsilon_2 + i\sigma_2)R^{20}$ for $L_r/L_d = 0.1$ (1), 0.2 (2), 0.3 (3), 0.01 (4), 0.02 (5) and 0.03 (6) (a) in the geometrical optics approximation (solid curves) and dependences of the relative error of calculation of the average radiation intensity at the first aberration maximum (b) and on the beam axis (c) on the diffraction parameter.

coherent radiation. This is especially noticeable when radiation propagates in media with strong aberrations.

The aim of our further study is to improve the method of diffraction rays by taking into account the fluctuations of the permittivity of a medium.

References

1. Belinskii A V, Chirkin A S *Opt. Atmos. Okean.* **4** 272 (1991)
2. Nazarathy M, Shamir J J. *Opt. Soc. Am.* **72** 1398 (1982)
3. Ratowsky R P, London R A *Phys. Rev A* **51** 3261 (1995)
4. Collins S A, Jr. *J. Opt. Soc. Am.* **60** 1168 (1970)
5. Klyukach I L, Sokolovskii R I *Zh. Eksp. Teor. Fiz.* **71** 424 (1976)
6. Bespalov V I, Pasmanik G A *Dokl. Akad. Nauk SSSR* **210** 309 (1973)
7. Marcuse D *Integrated Optics* (New York: IEEE Press, 1973; Opticheskie volnovody, Moscow: Mir, 1974)

8. Akhmanov S A, D'akov Yu E, Chirkin A S *Vvedenie v statisticheskuyu radiofiziku i optiku* (Introduction to Statistical Radiophysics and Optics) (Moscow: Nauka, 1981)
9. Feit M D, Fleck J A, Jr. *J. Opt. Soc. Am.* **7** 2048 (1990)
10. Ladagin V K, Starikov F A, Ustin V D *Kvantovaya Elektron.* **20** 471 (1993) [*Quantum Electron.* **23** 406 (1993)]
11. Starikov F A *Kvantovaya Elektron.* **24** 691 (1997) [*Quantum Electron.* **27** 673 (1997)]
12. Dudorov V V, Klosov V V *Proc. SPIE-Int. Soc. Opt. Eng.* **3983** 154 (1999)
13. Kravtsov Yu A, Orlov Yu *Geometricheskaya optika nednorodnykh sred* (Geometrical Optics of Inhomogeneous Media) (Moscow: Nauka, 1980)
14. Dudorov V V, Kolosov V V *Kvantovaya Elektron.* **28** 115 (1999) [*Quantum Electron.* **29** 672 (1999)]
15. Dudorov V V, Kolosov V V *Proc. SPIE-Int. Soc. Opt. Eng.* **4341** 218 (2000)
16. Hazak G, Bar-Shalom A *Phys. Rev. A* **38** 1300 (1988)
17. Dudorov V V, Kolosov V V *Opt. Atmos. Okean.* **10** 1561 (1997)